The 11th Canadian Conference on Earthquake Engineering
Canadian Association for Earthquake Engineering

# SYSTEM- VERSUS COMPONENT-LEVEL DUCTILITY CAPACITY OF REINFORCED CONCRETE BLOCK STRUCTURAL WALLS

**ABDELRHMAN OKASHA**
Teaching Assistant, the British University in Egypt, Egypt.
abdelrhman.okasha@bue.edu.eg

**MARWAN SHEDID**
Assistant Professor, AinShams University, Egypt.
marwan.shedid@eng.asu.edu.eg

**WAEL EL-DAKHAKHNI**
Martini, Mascarin and George Chair in Masonry Design, McMaster University, Canada.
eldak@mcmaster.ca

**ABSTRACT:** Most reinforced concrete block buildings are constructed of structural walls with different characteristics; as a result, under seismic loads such walls provide different responses which affect the overall response of the building. The primary aim of this paper is to assess the effect of the interaction between walls with different characteristics on the ductility capacity of the building. Such an assessment will lead to an important verdict about whether or not ignoring the system level interaction of individual walls will influence the value of the force modification factor of the entire system, thus, affecting the estimation of the total design base shear. In order to fulfil the aim of this study, a detailed comparison between evaluated displacement ductility values at component level and system level is presented in this paper. Results showed that for buildings constructed of different walls, the system level interaction of the walls significantly affect the displacement ductility of the system. Furthermore, it was found that in some cases buildings attained high displacement ductility values even higher than the value corresponding to the wall with highest displacement ductility in the system.

## 1. Introduction

The current National Building Code of Canada (NBCC) adopts force modification factor (R*)* to determine seismic design forces. The R factor represents the global ductility and overstrength of any seismic force resisting system (SFRS). Therefore, in order to obtain the *R* factor both ductility-related ($R_d$) and overstrength-related ($R_o$) force modification factors have to be evaluated (NBCC 2010). The NBCC (2010) introduces the equal-displacement approach to evaluate the factor $R_d$; however, a statistical approach is used to evaluate the factor $R_o$ (Mitchell et al. 2003). All the current design provisions provide $R_d$ values for structural walls based on evaluating the ductility capacity for different individual structural walls. However, what really decrees the level of the attracted seismic loads is the period of the entire building as a system. Consequently, accurately evaluating the ductility capacity at system level is quite essential to be capable of accurately estimating the design base shear for the entire system.

Many studies (Shedid et al. 2009, 2010a, 2011) have been established to relate between the response of individual reinforced concrete block shear walls and the overall response of reinforced concrete block building SFRS. These studies showed that in case of buildings that comprise structural walls with similar or close characteristics, the overall response of the building will be basically a scaled up response of the individual walls with the same basic behavioural characteristics (i.e., ductility capacity and strength degradation). Yet, when it comes to buildings which are constructed with structural walls that have different characteristics (i.e., aspect ratio, shape of cross section and reinforcement ratio) the overall response of the building will be much more sophisticated (Paulay 2000). At this particular case, the ductility capacity of each individual wall will not represent that of the entire system; hence, estimating the total design base shear based on the component level ductility capacity will be

spurious. This shows a major flaw in the current force-based seismic design approaches adopted by many provisions regarding accurately estimating the design base shear.

Eventually, this paper will focus on evaluating the effect of the interaction between reinforced-concrete block structural walls with different ductility capacities on the global ductility capacity of the building through comparing the obtained displacement ductility at component level with that obtained at system level. This study is divided into two major phases as follows: Phase I, which is generating experimentally verified finite element models for different reinforced concrete block walls and then evaluating the displacement ductility for each wall, and Phase II, which is utilizing the models created in the previous phase to generate another analytical models that represent different buildings and then evaluate the displacement ductility for each building. As previously stated, the analytical models generated in the first phase are verified based on an experimental study by Siyam (2015). The earlier experimental study reported by Siyam (2015) involved testing of third-scale rectangular and flanged reinforced concrete block structural walls under cyclic loading. Additionally, the testing matrix involved walls with different aspect ratios that range from 1.4 to 4.6. Further details and specifications regarding the experimental program are presented in the next section.

## 2. Experimental program

The experimental program was mainly intended for studying the flexural behaviour of third-scale reinforced concrete block structural walls under reversed cyclic loading. The test matrix consisted of various shear walls such as; rectangular slender and squat walls, C-shaped and slab-coupled walls (Siyam 2015). However, the first phase of this study is mainly dedicated for simulating the behaviour of rectangular slender walls only, accordingly, only the results of the rectangular slender walls will be shown below.

### 2.1. Test matrix

The table below (Table 1) shows walls type, aspect ratios, dimensions and reinforcement details. Bar diameter for vertical and horizontal reinforcement are donated by $\phi_v$ and $\phi_h$ respectively and the ratios of the vertical and horizontal reinforcement ratios are donated by $\rho_v$ and $\rho_h$ respectively.

The figure below (Fig. 1) shows the layout of each shear wall, each wall is two storeys where a slab is located at each storey level. Walls are built on same concrete foundations with the given dimensions in Fig. 1. The reinforcement layout for each shear wall is shown in Fig. 2. Horizontal reinforcement were hooked to the outermost vertical bars and they were placed at spacing equals to 65 mm in the first storey and 133 mm in the second storey resulting in horizontal reinforcement ratios equal to 0.26% and 0.14% as shown in Table 1.

**Table 1 – Walls type, dimensions and reinforcement details.**

| ID. | Type | Length (mm) | Height (mm) | Vertical reinforcement | | Horizontal reinforcement | | | Aspect ratio |
|---|---|---|---|---|---|---|---|---|---|
| | | | | $\phi_v$ (mm) | $\rho_v$ % | $\phi_h$ (mm) | $\rho_{h1}$ % | $\rho_{h2}$ % | |
| W3 | Rectangular | 598 | 2160 | 7.6 | 0.59 | 3.8 | 0.26 | 0.14 | 3.6 |
| W5 | Rectangular | 465 | 2160 | 7.6 | 0.61 | 3.8 | 0.26 | 0.14 | 4.6 |

### 2.2. Materials

Reduced-scale block were used in the constructions of the walls. The typical block has 130 mm length, 63.33 mm width and 65 mm depth. In order to get the compressive strength of fully grouted masonry, 24 prism specimens were tested and it was found that the average compressive strength is 19.25. The average young's modulus is 10.6 GPa based on the stress-strain relationship. Deformed D7 (7.6 mm) bars were used as vertical reinforcement, while, smooth W1.7 (3.8 mm) bars were used as horizontal reinforcement. The average yield strength of scaled bars was 495 MPa (Siyam 2015).

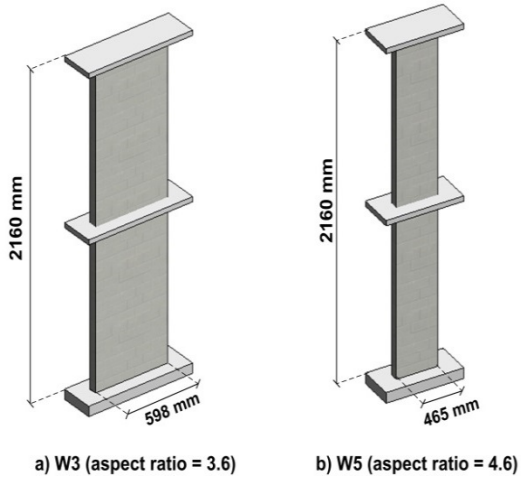


**Fig. 1 – Walls layout and dimensions.**

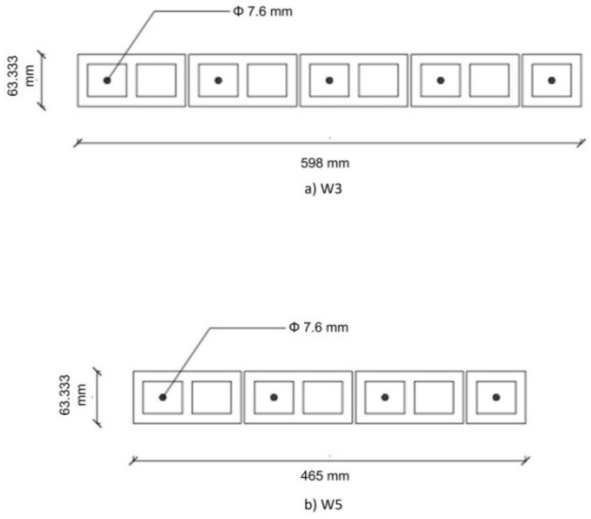


**Fig. 2 – Layout and reinforcement details.**

## 3. Phase I: Component Level

The first phase of this study is mainly devoted for evaluating the ductility capacity for different reinforced concrete block walls after simulating the nonlinear response of these walls using finite element models. Primarily, the first analytical models will be created and verified based on specimens W3 and W5. Afterwards, other models will be created using the same models for walls W3 and W5 but with increased reinforcement ratio and axial load ratio (ALR) to obtain different responses and then evaluate the displacement ductility at component level for all walls.

### 3.1. Analytical Model

An open source nonlinear structural analysis software OpenSees is used for simulating the nonlinear response of the reinforced concrete block structural walls. OpenSees is finite element software which was developed at the University of California, Berkely mainly for seismic analysis (McKenna et al. 2013). At this juncture, it is required to create analytical models based on specimens W3 and W5 shown previously.

#### 3.1.1. Element and Section Formulation

OpenSees flexure-shear interaction displacement-based beam-column element is used to develop two dimensional (2D) models that simulate the reinforced concrete block structural walls. Basically, displacement-based beam-column element follows the standard finite element formulation where section deformations are interpolated from an approximated displacement field. The formulation of this element assumes constant axial deformation and linear curvature distribution along the element length in order to approximate the nonlinear response (OpenSees 2006). Therefore, fine meshing of the element is necessary to accurately capture higher order distributions of deformations (Terzic 2011). The fiber section is divided into smaller regions that discretely model the reinforcement and concrete blocks regions, then, each material stress-strain response is integrated to simulate the overall behaviour of the wall. The discretization of the fiber section along with the choice of element length is discussed later.

#### 3.1.2. Constitutive Material Model

OpenSees material library comprises a wide range of material models; however, there is no material model which is mainly intended for concrete blocks. Instead, a uniaxial Concrete06 material model in OpenSees was used to simulate the behaviour of concrete blocks. The parameters required to define the material model are compressive strength (fc), strain at compressive strength (e0), compressive shape factor (n), post-peak compressive shape factor (k), tensile strength (fcr), tensile strain at peak stress (ecr) and exponent of the tension stiffening curve (b), (see Fig. 3). The stress-strain behaviour shown in Fig. 3 is mainly defined as the Thorenfeldt-base curve which is quite similar to the definition initially suggested by Popovics (1973), (OpenSees 2006):

$$\sigma_c = f'_c \frac{n\,(\frac{\epsilon c}{\epsilon 0})}{n-1+(\frac{\epsilon c}{\epsilon 0})^{nk}} \quad (1)$$

The tensile envelope curve utilizes the equation adopted for tension stiffening by Belarbi and Hsu (1994) but with a general exponent b (OpenSees 2006).

$$\epsilon c \leq \epsilon cr,\ \sigma_c = \left(\frac{fcr}{\epsilon cr}\right) \epsilon c \quad (2)$$

$$\epsilon c > \epsilon cr,\ \sigma_c = fcr\ \left(\frac{\epsilon cr}{\epsilon c}\right)^b \quad (3)$$

An isotropic nonlinear material model, Steel02, is used to create a uniaxial Giuffre-menegotta-Pinto steel material to model the steel reinforcement in this study (Menegotto and Pinto 1973; OpenSees 2006). The required parameters to define the material model are yield strength (Fy), initial elastic tangent (E), strain hardening ratio (b) which is the ratio between post-yield tangent and initial elastic tangent and a constant parameters (R0) with a recommended value equals to 20, (Fig. 4). The relation between the non-dimensional stress and strain based on the Giuffre-Menegotto-Pinto model is given by:

$$\sigma^* = b\epsilon^* \frac{(1-b)\epsilon^*}{(1+\epsilon^{*R})^{1/R}} \quad (4)$$

As shown in Fig. 4 the material model used to simulate the reinforcement steel does not consider fracture strain. As a result, the MinMax material is used to define fracture strain for steel fibers in the model. In this study all the parameters used to define concrete and steel material models are based on either the test results of the materials used in the experimental program or model calibration according to the experimental data.

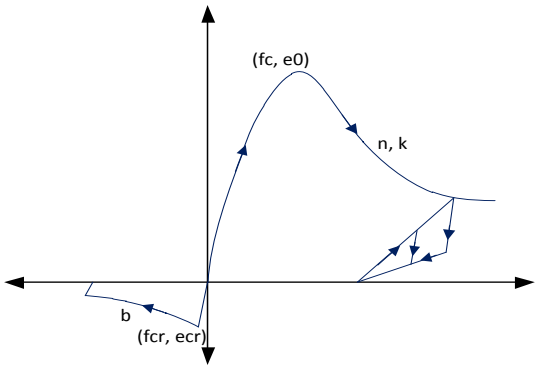


**Fig. 3 – Stress-strain curve for concrete.**

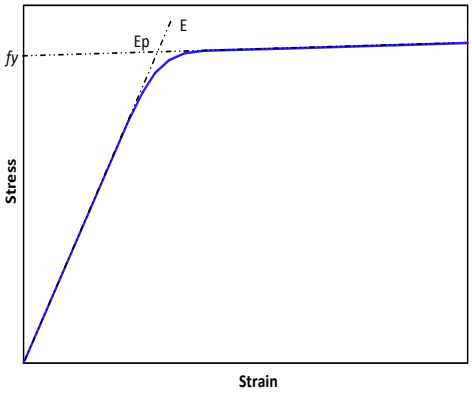


**Fig. 4 – Stress-strain curve for steel.**

### 3.1.3. Nonlinear Modelling Approach

As stated earlier, each wall is represented using displacement-based beam-column elements, and each element has an assigned fiber section which comprises a stack of fibers where each fiber represents either a grouted concrete block or a steel bar. The arrangement of fibers in each element section for both models (W3 and W5) is shown in Fig. 5. The major aspects that highly influence the resultant behaviour from the finite element model when using displacement-based beam-column elements are the choice of elements lengths along the height of the wall and the number of integration points. Due to strain localization which takes place at the base of the wall, it is essential to attain fine meshing along the region of plastic deformations. In essence, the analytical results are very sensitive to the choice of elements lengths along the length of the plastic hinge. According to a recent study by Ezzeldin et al. (2014), the recommended initial values for elements lengths are between 20% and 50% the length of the wall and using five integration points for each element. The most optimum elements lengths were attained through continuous tuning of the model after comparing the analytical results to the experimental data. Since, this study is not mainly intended for evaluating the sensitivity of analytical results to elements lengths, therefore, the final choice of elements lengths along with the general layout for both W3 and W5 models are shown in Fig. 6. Eventually, axial loads which include weight of the loading beam and self-weight were applied to the wall, then, monotonic pushover horizontal displacements were applied at the top of the wall using the displacement control.

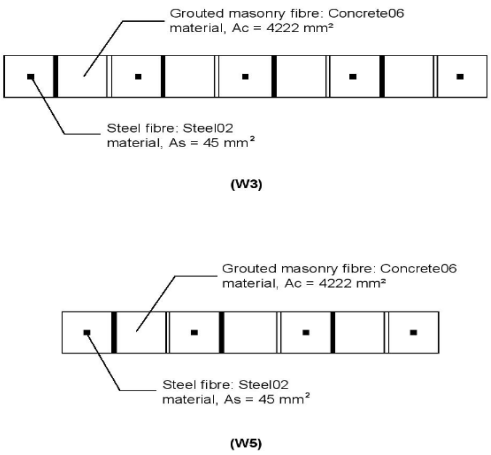


Fig. 5 – Fibers layout in cross section.

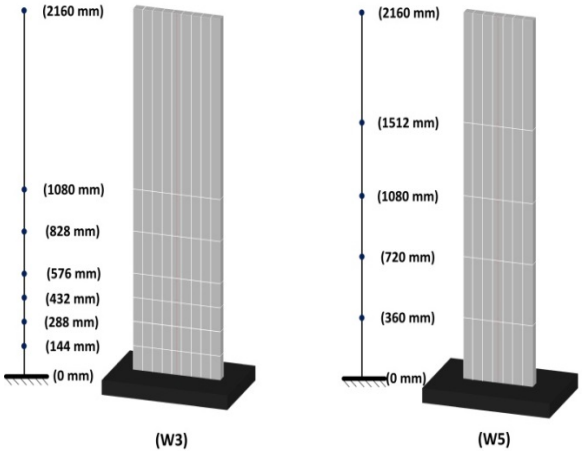


Fig. 6 – General layout of analytical models.

### 3.2. Comparison between Analytical and Experimental Results

The analytical load-displacement results for walls W3 and W5 are compared to the experimentally measured average cyclic envelope response for both walls (Fig. 7). The figures below show good agreement between experimental and analytical results using OpenSees, which, indicates that the finite element models are capable of capturing the main characteristics of the actual nonlinear response for both walls. Table 2 shows the obtained analytical and experimental ultimate capacity ($Q_u$), displacement at first yield ($\Delta_y$), displacement at ultimate capacity ($\Delta_u$) and displacement at 20% strength degradation ($\Delta_{0.8u}$) for both walls.

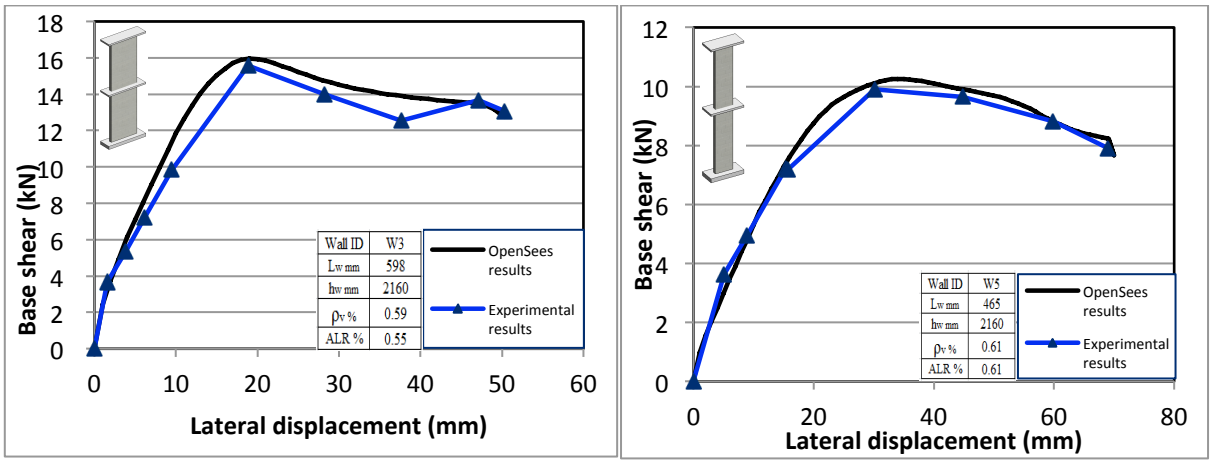


(a) W3 (b) W5

Fig. 7 – Experimental and analytical results for walls W3 and W5.

Table 2 – Comparison between experimental and analytical results.

| ID. | Δy Exp. (mm) | Δy Anl. (mm) | Δu Exp. (mm) | Δu Anl. (mm) | Δ0.8u Exp. (mm) | Δ0.8u Anl. (mm) | Qu Exp. (kN) | Qu Anl. (kN) |
|---|---|---|---|---|---|---|---|---|
| W3 | 9.5 | 9.75 | 19.6 | 19 | 53.65 | 50.34 | 15.58 | 15.96 |
| W5 | 13.8 | 13.54 | 30 | 34 | 69 | 69.1 | 9.9 | 10.26 |

### 3.3. Models with High Axial Load ratio and Reinforcement ratio

Many previous experimental studies (Zhang and Wang 2000; Su and Wong 2007; Shedid et al. 2008; Jiang et al. 2013) evaluated the effect of ALR and reinforcement ratio on the ductility of shear walls. These studies stated that increasing ALR and reinforcement ratio leads to significant reduction in the ductility capacity of shear walls. After being confident that the primary analytical models can simulate

the nonlinear behaviour of the walls, secondary models were generated based on the primary models but with significant increase in ALR and reinforcement ratio to attain different responses with different ductility capacities. For wall W3 the ALR increased from 0.55% to 4.15%, while, for wall W5 ALR and reinforcement ratio increased from 0.61% to 8.9% and 1.06% respectively (Table 3). The analytical results of these models are shown below (Fig. 8) compared to the results of the primary models.

**Table 3 – Walls dimensions, reinforcement and axial load ratios for secondary models.**

| ID. | Length (mm) | Height (mm) | $\rho_v$ % | ALR % |
|---|---|---|---|---|
| W3-1 | 598 | 2160 | 0.59 | 4.15 |
| W5-1 | 465 | 2160 | 1.06 | 8.9 |

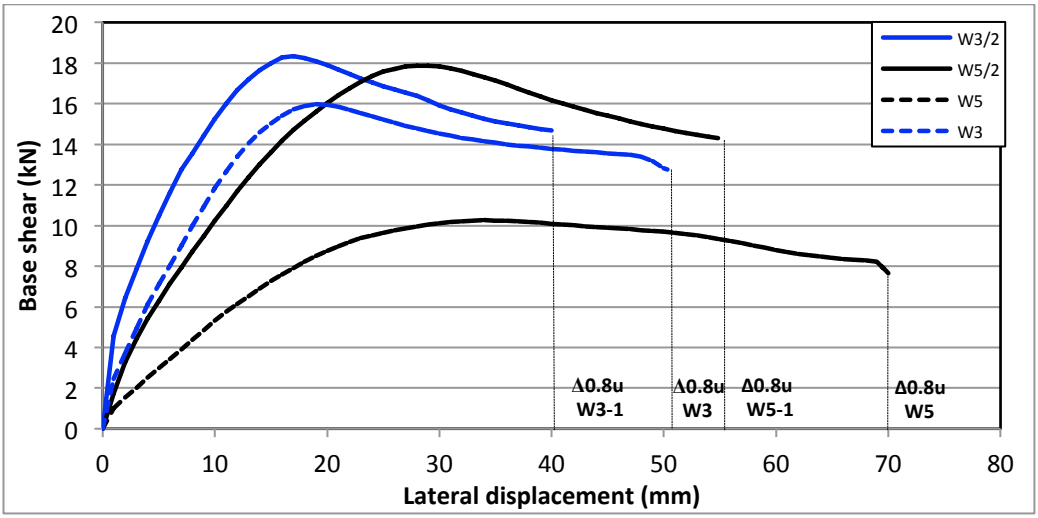


**Fig. 8 – Analytical results for primary and secondary models.**

### 3.4. Displacement Ductility at Component Level

The nonlinear load-displacement relationship obtained from static analysis must be idealized to a bilinear model to be capable of establishing a common procedure to evaluate the displacement ductility (μ), (Shedid et al. 2010b). There are many idealization approaches in the literature; however, the scope of this study is not to distinguish between different idealization approaches. The idealization technique used in this study was suggested by Tomazevic (1998) which is based on equating the area under the obtained and idealized curves of the load-displacement relationship to get the idealized yield displacement ($\Delta^{ep}$) for the bilinear curve with initial elastic stiffness ($k_e$) and selected ultimate performance displacement (Fig. 9). The elastic stiffness is the ratio between yield capacity and the corresponding displacement ($Q_y/\Delta_y$). Afterwards, in order to evaluate the value of μ, the ultimate performance displacement of shear walls must be determined. It has been widely accepted among researchers (Priestly et al. 1996; Priestley et al. 2007; ATC-63 2008) that the ultimate performance displacement is corresponding to 20% strength degradation ($\Delta_{0.8u}$). The $\mu^{ep}_{\Delta 0.8u}$ value is then equal to the ratio between $\Delta_{0.8u}$ and $\Delta_{ep}$ (Fig. 9). The values for $\mu^{ep}_{\Delta 0.8u}$ for each wall are listed in Table 4.

**Table 4 – Summary of the obtained displacements and calculated displacement ductilities.**

| ID. | $Q_y$ (kN) | $\Delta_y$ (mm) | $Q_u$ (kN) | $\Delta_u$ (mm) | $\Delta^{ep}$ (mm) | $\Delta_{0.8u}$ (mm) | $\mu^{ep}_{\Delta 0.8u}$ |
|---|---|---|---|---|---|---|---|
| W3 | 11.62 | 9.75 | 15.96 | 19 | 12.3 | 50.34 | 4.09 |
| W3-1 | 14.31 | 8.87 | 18.34 | 17 | 10.6 | 40 | 3.77 |
| W5 | 6.739 | 13.54 | 10.26 | 34 | 19.2 | 69.1 | 3.6 |
| W5-1 | 13.56 | 14.92 | 17.88 | 29 | 18.4 | 54.85 | 2.98 |

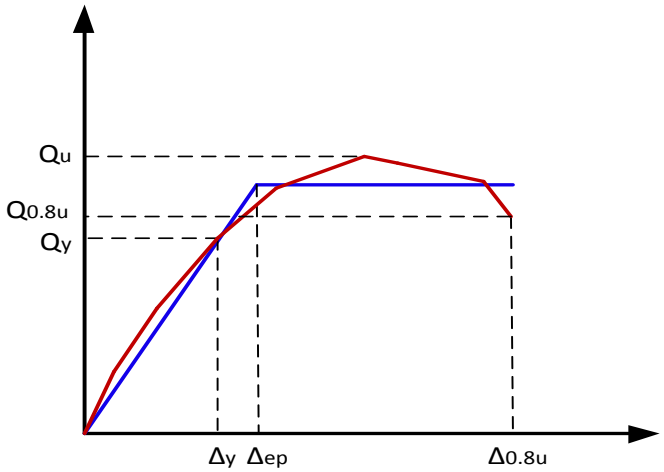


**Fig. 9 – Idealized elastic plastic response.**

## 4. Phase II: System Level

The aim of the second phase of this study is to evaluate displacement ductility for different reinforced concrete block buildings. Several analytical models will be created that represent different buildings which utilize the finite element models created in the previous phase as the main SFRS. Subsequently, the ductility capacity will be assessed after obtaining the overall nonlinear response of these buildings.

### 4.1. Analytical Models and Results

Currently, it is required to develop 2D analytical models for buildings which comprise different structural walls. The scheme of these models is that each building model will include four or five walls linked with a rigid diaphragm; however, the major concern at this point is the choice of walls in each building. The main criteria of assigning walls in each building is first ensuring that there will be good distribution of strength contribution among shear walls in each building so there will be no dominant shear wall in the building that governs the overall response of the system and second to achieve different average displacement ductility values for all buildings. The general scheme of a typical analytical model and the layout of each building model are presented in Fig. 10 and Table 5 respectively. The effect of rigid diaphragm is simulated using equal DOF command in OpenSees to ensure that all structural walls will maintain the same lateral displacement at the top node on each step. Monotonic pushover horizontal displacements were applied at the top of the building using the same loading protocol as the previous phase. Fig. 11 shows the analytical results of each building.

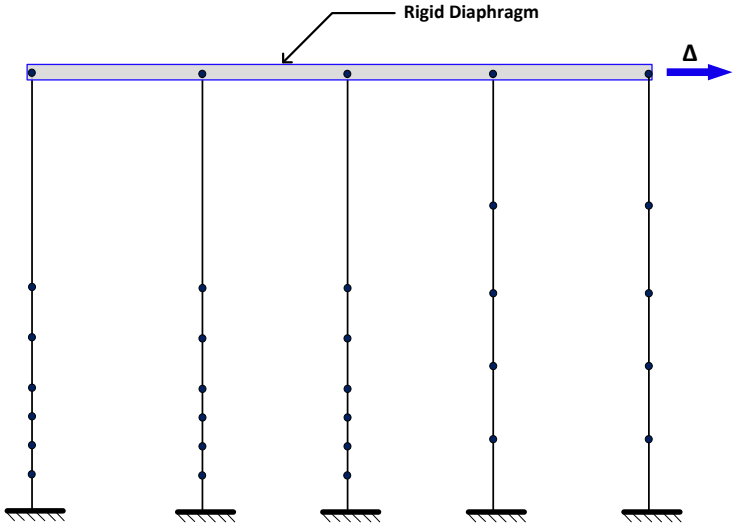


**Fig. 10 – General layout of system level analytical models.**

**Table 5 – General layout of system level analytical models.**

| System Models | Component Models | | | | |
|---|---|---|---|---|---|
| | 1 | 2 | 3 | 4 | 5 |
| **BM 1** | W 5-1 | W 5 | W 5 | W 3-1 | W 3 |
| **BM 2** | W 5 | W 5 | W 3-1 | W 3 | W 3 |
| **BM 3** | W 5-1 | W 3 | W 3 | W 3 | W 3 |
| **BM 4** | W 5-1 | W 5-1 | W 3-1 | W 3-1 | - |
| **BM 7** | W 5-1 | W 3-1 | W 3-1 | W 3-1 | - |
| **BM 8** | W 5 | W 5 | W 3-1 | W 3-1 | W 3-1 |

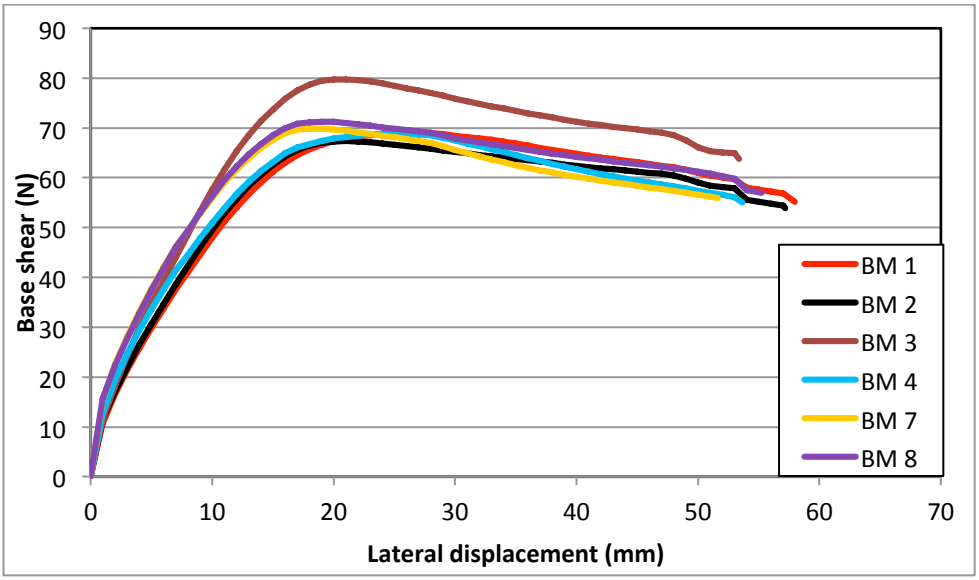


**Fig. 11 – Analytical results for system level models.**

## 4.2. Displacement Ductility at System Level

The ductility capacity of the building is assessed using the same approach used to evaluate that of individual structural walls as shown in the previous phase. However, the main issue regarding using the same approach for evaluation is that the earlier idealization approach used to compute the displacement ductility requires identifying the elastic stiffness which is simple for individual elements as it is taken at first yield but much more complex for an entire building that includes different walls with different yielding levels. In order to overcome this issue it was assumed that the yield of the building will occur at 80% of the ultimate capacity of the entire building. A verification model was generated to attest the validity of this assumption. The verification model is for a building that comprises five similar structural walls (W3) with $\mu^{ep}_{\Delta 0.8u}$ value equals to 4.09 and it was found that $\mu^{ep}_{\Delta 0.8u}$ value of the building, based on the assumption mentioned above, was 3.91 which is 4.4% less than the exact value (Fig. 12). Therefore, the displacement ductility for all buildings are evaluated using the same approach used previously but assuming that $Q_y = Q_{0.8u}$. Table 6 summarizes the obtained values for the ultimate and yield capacities and displacements for each building; furthermore, values of $\mu^{ep}_{\Delta 0.8u}$ for each building are listed in Table 7.

**Table 6 – Summary of capacities and displacement ductilities for system level models.**

| Building ID | Qy Sys. (kN) | Qu Sys. (kN) | Δy Sys. (mm) | Δu Sys. (mm) |
|---|---|---|---|---|
| BM 1 | 55.20 | 69.00 | 12.44 | 27.00 |
| BM 2 | 53.87 | 67.34 | 11.35 | 21.00 |
| BM 3 | 63.81 | 79.77 | 11.60 | 21.00 |
| BM 4 | 55.07 | 68.84 | 11.41 | 25.00 |
| BM 7 | 55.886 | 69.857 | 9.96 | 18 |
| BM 8 | 56.981 | 71.226 | 10.19 | 19 |

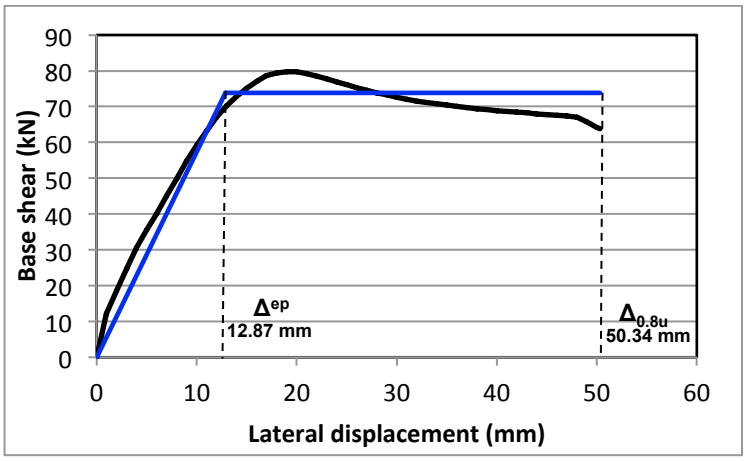


**Fig. 12 – The nonlinear and idealized responses for the verification model.**

## 5. Comparison between System and Component Level Displacement Ductility Values

In order to assess the effect of interaction between different structural walls on the global ductility capacity of the system it is quite substantial to correlate the displacement ductility evaluated at system level to component level. As shown in Table 7 the values of $\mu^{ep}_{\Delta 0.8u}$ for all systems are inconsistent, the values are from 1.5 to 23 percent higher than the weighted average value of $\mu^{ep}_{\Delta 0.8u}$, it is sum of $\mu^{ep}_{\Delta 0.8u}$ for each wall in the system factored by its strength contribution, which indicates that the effect of the interaction vary from one system to another. For building model BM 4, BM 7 and BM 8 the values of $\mu^{ep}_{\Delta 0.8u}$ are around 20% higher than the weighted average value. Moreover, the displacement ductility of these buildings are 5, 17 and 22 percent higher than the maximum value of $\mu^{ep}_{\Delta 0.8u}$ in each system respectively. In essence, these figures indicate that some systems gained significant increase in ductility capacity due to the interaction between different structural walls with significant difference in $\Delta_y$ and $\Delta_{0.8u}$. For instance, for a building that comprises four similar walls (W3-1) the evaluated $\mu^{ep}_{\Delta 0.8u}$ for this system using same approach mentioned previously is 3.67 which is 2.7% less than the exact value 3.77. However, when exchanging only one wall in the system with wall W5-1 as shown in building BM 7, which has a significantly different $\Delta_y$ and $\Delta_{0.8u}$, the value of $\mu^{ep}_{\Delta 0.8u}$ massively increase to 4.42. Buildings BM 1 and BM 2 show $\mu^{ep}_{\Delta 0.8u}$ values around 10% higher than the weighted average value and the value for BM 2 is 4% higher than the maximum value of $\mu^{ep}_{\Delta 0.8u}$ in the system. Building BM 3 has a displacement ductility close the weighted average value because $\Delta_y$ and $\Delta_{0.8u}$ of the system are close to average values.

## 6. Conclusion

This paper aimed at evaluating the displacement ductility of reinforced concrete block buildings constructed with different structural walls to investigate the effect of system level interaction of the structural walls on the ductility capacity of the building. Several analytical models were created and verified based on experimental data to represent individual structural walls. Afterwards, these analytical models were utilized to create analytical models that represent different buildings. A comparison between the building's and individual walls' behaviours were presented in terms of the displacement ductility; this comparison highlighted the effect of system level interaction of different walls in the system. The following conclusions were reached based on the detailed analysis presented in this paper.

It was found from the comparison between system and component level responses that in case of buildings constructed with different walls it cannot be assumed that the displacement ductility value of any wall in the building can represent that of the system. The values of displacement ductility values of the buildings varied significantly depending on the variation of yield and ultimate performance displacements of the individual walls in the system. The values of displacement ductility values at system level were 1.5% to 23% higher than the weighted average value for walls in each system. Moreover, some buildings showed displacement ductility values higher than the maximum component value in the system which indicated that some buildings maintained displacement ductility values higher than that of individual walls in the system through system level interaction between the walls. Eventually, it is important to draw attention towards the fact that designing individual structural walls while disregarding their system level interaction in the system will inevitably lead to inaccurate design.

***Table 7* – System and component displacements and displacement ductilities.**

| Building ID | Walls ID. | Strength contribution % | $\Delta^{ep}$ Sys. (mm) | $\Delta_{0.8u}$ Sys. (mm) | $\mu^{ep}_{\Delta 0.8Fu}$ Comp. | $\mu^{ep}_{\Delta 0.8Fu}$ Sys. | $\mu^{ep}_{\Delta 0.8Fu}$ Average | $\mu^{ep}_{\Delta 0.8Fu}$ Weighted Average |
|---|---|---|---|---|---|---|---|---|
| BM 1 | W 5-1 | 25.83% | 14.9 | 57.97 | 2.98 | 3.9 | 3.608 | 3.587 |
| | W 5 | 14.29% | | | 3.6 | | | |
| | W 5 | 14.29% | | | 3.6 | | | |
| | W 3-1 | 23.96% | | | 3.77 | | | |
| | W 3 | 21.62% | | | 4.09 | | | |
| BM 2 | W 5 | 13.36% | 13.5 | 57.20 | 3.6 | 4.24 | 3.83 | 3.88 |
| | W 5 | 13.36% | | | 3.6 | | | |
| | W 3-1 | 26.25% | | | 3.77 | | | |
| | W 3 | 23.52% | | | 4.09 | | | |
| | W 3 | 23.52% | | | 4.09 | | | |
| BM 3 | W 5-1 | 20.58% | 13.6 | 53.38 | 2.98 | 3.92 | 3.868 | 3.86 |
| | W 3 | 19.85% | | | 4.09 | | | |
| | W 3 | 19.85% | | | 4.09 | | | |
| | W 3 | 19.85% | | | 4.09 | | | |
| | W 3 | 19.85% | | | 4.09 | | | |
| BM 4 | W 5-1 | 25.52% | 13.6 | 53.66 | 2.98 | 3.96 | 3.375 | 3.37 |
| | W 5-1 | 25.52% | | | 2.98 | | | |
| | W 3-1 | 24.48% | | | 3.77 | | | |
| | W 3-1 | 24.48% | | | 3.77 | | | |
| BM 7 | W 5-1 | 21.70% | 11.7 | 51.63 | 2.98 | 4.42 | 3.5725 | 3.60 |
| | W 3-1 | 26.10% | | | 3.77 | | | |
| | W 3-1 | 26.10% | | | 3.77 | | | |
| | W 3-1 | 26.10% | | | 3.77 | | | |
| BM 8 | W 5 | 11.94% | 12.1 | 55.25 | 3.6 | 4.58 | 3.702 | 3.73 |
| | W 5 | 11.94% | | | 3.6 | | | |
| | W 3-1 | 25.37% | | | 3.77 | | | |
| | W 3-1 | 25.37% | | | 3.77 | | | |
| | W 3-1 | 25.37% | | | 3.77 | | | |

## 7. References


Applied Technology Council (ATC), "Quantification of Building Seismic Performance Factors", *ATC-63 Project Rep.,* Applied Technology Council, Redwood City, Calif, 2008.

BELARBI, Abdeldjelil, HSU, Thomas, "Constitutive Laws of Concrete in Tension and Reinforcing Bars Stiffened by Concrete", *ACI Structural Journal*, Vol. 91, No. 4, July 1994, pp. 465-474.

EZZELDIN, Mohamed, WIEBE, Lydell, SHEDID, Marwan, EL-DAKHAKHNI, Wael, "Numerical Modelling of Reinforced Concrete Block Structural Walls Under Seismic Loading", *9th International Masonry Conference, Guimaraes*, July 2014.

JIANG, Huanjun, WANG, Bin, LU, Xilin, "Experimental Study on Damage Behavior of Reinforced Concrete Shear Walls Subjected to Cyclic Loads", *Journal of Earthquake Engineering*, Vol. 17, No. 7, September 2013, pp. 958-971.

MCKENNA, Frank, FENVES, Gregory, SCOTT, Michael, Open System for Earthquake Engineering Simulation, *University of California, Berkeley, CA,* Retrieved from: http://opensees.berkeley.edu, Version 2.4.3, November 2013.

MENEGOTTO, Marco, PINTO, Paolo, "Method of Analysis for Cyclically Loaded R.C. Plane Frames Including Changes in Geometry and Non-Elastic Behavior of Elements Under Combined Normal Force and Bending", *IABSE Symposium on Resistance and Ultimate Deformability of Structures Acted on by Well Defined Repeated Loads, Lisbon*, 1973, pp. 15-22.

MITCHELL, Denis, TREMBLAY, Robert, KARACABEYLI, Erol, PAULTRE, Patrick, SAATCIOGLU,

Murat, ANDERSON, Donald, “Seismic Force Modification Factors for the Proposed 2005 Edition of the National Building Code of Canada”, *Canadian Journal of Civil Engineering*, Vol. 30, No. 2, April 2003, pp. 308-327.

National Building Code of Canada (NBCC), 2010, Institute for Research in Construction, National Research Council of Canada, Ottawa, ON, Canada.

OpenSees, OpenSees Command Language Manual, 2006.

PAULAY, Tom, “A Simple Displacement Compatibility-Based Seismic Design Strategy for Reinforced Concrete Buildings”, *12th World Conference on Earthquake Engineering*, February 2000.

POPOVICS, Sándor, “A Numerical Approach to the Complete Stress-Strain Curve of Concrete”, *Cement and Concrete Research*, Vol. 3, No. 4, 1973, pp. 583-599.

PRIESTLEY, Michael, SEIBLE, Frieder, CALVI, Gian, “Seismic Design and Retrofit of Bridges”, *Wiley, New York*, 1996.

PRIESTLEY, Michael, CALVI, Gian, KOWALSKY, Mervyn, “Displacement-Based Seismic Design of Structures”, *IUSS, Pavia, Italy*, May 2007.

SHEDID, Marwan, EL-DAKHAKHNI, Wael, DRYSDALE, Robert, “Behavior of Fully Grouted Reinforced Concrete Masonry Shear Walls Failing in Flexure: Analysis”, *Engineering Structures*, Vol. 31, No. 9, September 2009, pp. 2032-2044.

SHEDID, Marwan, EL-DAKHAKHNI, Wael, DRYSDALE, Robert, “Characteristics of Rectangular, Flanged, and End-Confined Reinforced Concrete Masonry Shear Walls for Seismic Design”, *Journal of Structural Engineering*, Vol. 136, No. 12, December 2010a, pp. 1471-1482.

SHEDID, Marwan, EL-DAKHAKHNI, Wael, DRYSDALE, Robert, “Seismic Response Modification Factors for Reinforced Masonry Structural Walls”, *Journal of Performance of Constructed Facilities*, Vol. 25, No. 2, April 2011, pp. 74-86.

SHEDID, Marwan, DRYSDALE, Robert, EL-DAKHAKHNI, Wael, “Behavior of Fully Grouted Reinforced Concrete Masonry Shear Walls Failing in Flexure: Experimental Results”, *Journal of Structural Engineering*, Vol. 134, No. 11, November 2008, pp. 1754-1767.

SHEDID, Marwan, EL-DAKHAKHNI, Wael, DRYSDALE, Robert, “Seismic Performance Parameters for Reinforced Concrete-Block Shear Wall Construction”, *Journal of Performance of Constructed Facilities*, Vol. 24, No. 1, February 2010b, pp. 4-18.

SIYAM, Mustafa, “Seismic Performance of Ductile Reinforced Masonry Shear Walls for Seismic Design”, *Ph.D. thesis, McMaster University, Hamilton, ON, Canada*, June 2015.

SU, R.K.L, WONG, S.M, “Seismic Behaviour of Slender Reinforced Concrete Shear Walls Under High Axial Load Ratio”, *Engineering Structures*, Vol. 29, No. 8, August 2007, pp. 1957-1965.

TERZIC, Vesna, “Force-Baed Elemnet vs. Displacement-Based Element”, *University of California, Berkeley, CA,* Retrieved from: http://opensees.berkeley.edu/wiki/images/2/26/FBEvsDBE final.pdf, December 2011.

TOMAZEVIC, Miha, “Earthquake-Resistant Design of Masonry Buildings”, *Imperial College Press, Covent Garden, London, UK*, 1998.

ZHANG, Yunfeng, WANG, Zhihao, “Seismic Behavior of Reinforced Concrete Shear Walls Subjected to High Axial Loading”, *ACI Structural Jounral*, Vol. 97, No. 5, September 2000, pp. 739-750.